

## ON FUNDAMENTAL OPERATING PRINCIPLES AND RANGE-DOPPLER ESTIMATION IN MONOLITHIC FREQUENCY-MODULATED CONTINUOUS-WAVE RADAR SENSORS

**Vladimir M. Milovanovic**

Faculty of Engineering  
University of Kragujevac

**Abstract.** *The diverse application areas of emerging monolithic noncontact radar sensors that are able to measure object's distance and velocity is expected to grow in the near future to scales that are now nearly inconceivable. A classical concept of frequency-modulated continuous-wave (FMCW) radar, tailored to operate in the millimeter-wave (mm-wave) band, is well-suited to be implemented in the baseline CMOS or BiCMOS process technologies. High volume production could radically cut the cost and decrease the form factor of such sensing devices thus enabling their omnipresence in virtually every field. This introductory paper explains the key concepts of mm-wave sensing starting from a chirp as an essential signal in linear FMCW radars. It further sketches the fundamental operating principles and block structure of contemporary fully integrated homodyne FMCW radars. Crucial radar parameters like the maximum unambiguously measurable distance and speed, as well as range and velocity resolutions are specified and derived. The importance of both beat tones in the intermediate frequency (IF) signal and the phase in resolving small spatial perturbations and obtaining the 2-D range-Doppler plot is pointed out. Radar system-level trade-offs and chirp/frame design strategies are explained. Finally, the nonideal and second-order effects are commented and the examples of practical FMCW transmitter and receiver implementations are summarized.*

**Key words:** *FMCW, frequency-modulated continuous-wave, radar, mm-wave, linear chirp, range-Doppler, sensors, radar-on-a-chip (RoC), single-chip radar.*

---

Received September 10, 2018

**Corresponding author:** Vladimir M. Milovanović

Department of Electrical Engineering, Faculty of Engineering, University of Kragujevac,

Sestre Janjic 6, 34000 Kragujevac, Serbia

(E-mail: vlada@kg.ac.rs)

## 1 INTRODUCTION

Applications of portable short-range contact-less radar sensors which provide simultaneous information on the presence, position and relative radial velocity are virtually countless. These radar systems not only have the potential to improve the service quality in numerous existing fields [1–3], but are also expected to be the driving force for many novel use-cases in the near future.

Multiple sensing technologies based on laser/optical, ultrasound and radio waves have been proposed in the past. Among those, the millimeter-wave (mm-wave) radio frequency radars attracted considerable attention thanks to their robustness [4] against bad weather conditions and harsh environments.

Historically, mm-wave radar sensors were built from discrete components and therefore reserved only for low-volume markets. However, a prospective single-chip integrated solution with a low unit cost and small form factor, often referred to as the radar-on-chip (RoC), would lead to its omnipresence in consumer and industrial electronic devices, along with probable pervasive use in a variety of areas spanning from automotive to healthcare.

Two fundamentally different microwave ranging methods, a pulse-based and continuous-wave (CW), coexist. The former ones are simply inefficient for monolithic integration [5], as they inherently suffer from higher peak(-to-average) power. Unmodulated CW radars can only determine the relative target velocity through the Doppler shift. Nevertheless, if the appropriate [6] kind of carrier modulation is employed, distances can also be resolved.

Pseudorandom noise modulated CW radars [7] that exploit pulse compression techniques for temporal energy distribution are a viable option especially for lower node digitally-intensive implementations [8], but come with a major drawback [9] that their baseband bandwidth equals half of the radio frequency (RF) one. This fact proves to be particularly bothersome in ultra-high resolution sensors where power-hungry data converters are unavoidable.

Finally, the classical frequency-modulated CW (FMCW) radar, as will be presented by this article, in its simplest homodyne incarnation, transmits a sequence of linear chirps that are simultaneously used as a local oscillator signal for the receiver's frequency mixer. Assuming no nonlinear distortions occur on the pathway, when the transmitted chirp is mixed with its received reflections that are attenuated, delayed in time and possibly shifted in frequency the intermediate frequency, being the low-pass filtered heterodyning product, will contain information on the target's distance (via time of flight) and its velocity (Doppler effect). By analogy with acoustics, the resulting frequency difference, at the mixer's output is referred to as the beat frequency.

Recently, the FMCW radars drew considerable attention [10–21], partially owing to their high integration potential. Although the main driver in developing these small footprint solutions was the automotive industry [1], a gradual breakthrough into other spheres is evident. Regulatory committees of the ITU and the ETSI even assigned the dedicated 77-81 GHz range in the W-band as part of the spectrum to be automotive specific, which is often referred to as the so-called “short-range radar” (SRR) band. In spite of that, having a device that could operate in the frequency band where an unlicensed spectral emission is permitted would be favorable for its widespread adoption. Namely, choosing one of the industrial, scientific, and medical (ISM) radio bands might turn out advantageous for cross-disciplinary expansion of FMCW-based sensors that will not be limited to vehicular radar systems.

The mm-wave radars can grasp important benefits of higher frequency operation that are not only related to its antenna size. As will be also shown in the next sections, the FMCW multitarget differentiation ability is directly proportional to the irradiated chirp bandwidth. In the prospect of the FCC’s relatively recent extension of the unlicensed part in the V band [22], that now incorporates a complete 57-71 GHz frequency range, previously unfeasible spatial target discrimination is enabled. In other words, these 14 GHz of a contiguous unlicensed spectrum translate to a centimeter-order space resolution, thus allowing FMCW-type radars to be used in complex indoor and outdoor scenes which contain an abundance of close proximity objects.

All this sets a fruitful ground for a universal ranging radar devices, which will dominate the future markets. The first commercial RoC solutions already appeared [23] and more are following and are expected to follow fairly soon.

This paper is intended to make a rather gentle introduction to the area of integrated FMCW mm-wave radar sensors as they are presently build. It focuses on main operating principles in estimating object distance/range and its relative radial velocity in sensor devices that are based on fast FMCW modulation and slow time processing which gives multiple advantages.

In order to follow the elaborated matter, a general undergraduate-level knowledge in electronics and signal processing is assumed. The rest of the paper is organized as follows. Concept of a frequency chirp as the fundamental signal in FMCW radars is introduced in Section 2. Further in Section 3 it is elaborated on the operating principles of FMCW sensors with two subsections each devoted to range and velocity estimation. Final subsection gives some system-level trade-offs and explains chirp/frame design decisions. Present state of the art FMCW radar transmitter and receiver architectures are examined in Section 4 and finally Section 5 concludes the article.

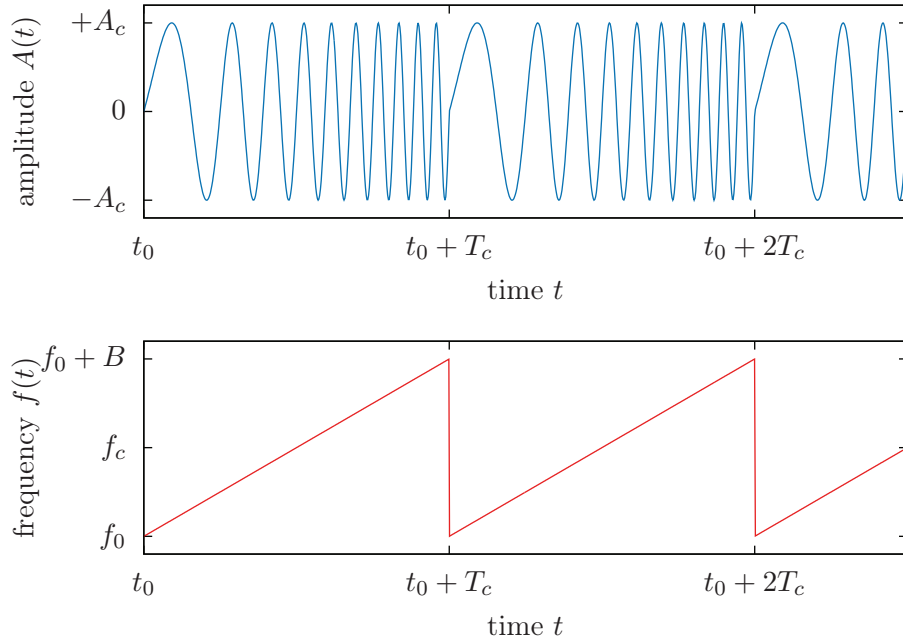


Fig. 1. A time sequence of linear up-chirp waveforms plotted as amplitude versus time (upper subplot) and frequency versus time (lower subplot) resembling the sawtooth wave.

## 2 CHIRP AS THE FUNDAMENTAL SIGNAL OF AN FMCW RADAR

A sine wave or a sinusoid whose frequency increases (up-chirp) and/or decreases (down-chirp) with time is called a chirp or, although less often in this context, a sweep. In particular, linear chirps, i.e. signals in which the frequency changes linearly with time, are at the heart of every FMCW radar.

Specifically, in a linear chirp, a representative example of which is plotted in Fig. 1, the instantaneous frequency  $f$  varies exactly linearly with time  $t$ :

$$f(t) = f_0 + \frac{B}{T_c}(t - t_0) = f_0 + S(t - t_0) \quad , \quad (1)$$

where  $f_0$  is the starting frequency at time point  $t = t_0$ , while  $S = B/T_c$  is the rate of frequency change or the frequency slope, sometimes also referred to as the chirpyness. The slope is defined using two parameters, namely the chirp bandwidth  $B$  and its duration  $T_c$ , also called the modulation time.

Since the time derivative of the phase  $\phi$  is the angular frequency, the corresponding time-domain function for the phase of any oscillating signal is the integral of the frequency function, and therefore the phase is expected to grow like  $\phi(t + \Delta t) \simeq \phi(t) + 2\pi f(t)\Delta t$  as a function of time. This results in:

$$\phi(t) = \phi_0 + 2\pi \int_{t_0}^t f(\tau) d\tau = \phi_0 + 2\pi \left[ f_0(t - t_0) + \frac{B}{2T_c}(t^2 - t_0^2) \right] \quad , \quad (2)$$

where  $\phi_0$  is the initial phase at time point  $t = t_0$ . Deriving the previous expression it can be verified that  $\phi'(t) = 2\pi f(t)$ , what was actually expected.

Finally, the corresponding time-domain function for a sinusoidal linear chirp is the sine of the quadratic-phase signal in radians and can be written:

$$y_c(t) = v_{\text{TX}}(t) = A_c \sin \left( \phi_0 + 2\pi f_0 t + \pi \frac{B}{T_c}(t - mT_c)^2 \right) \quad , \quad (3)$$

where  $A_c$  is the chirp's amplitude and where  $t_0 = 0$  under assumptions that the sweeps are performed continuously and that  $m$  represents the  $m^{\text{th}}$  chirp.

The carrier frequency can be defined in terms of the starting frequency and the modulation bandwidth as  $f_c = f_0 + B/2$  and represents the central frequency for the spectrum band that is being covered. Typical frequency bands of interest in the mm-wave part are around 64 GHz for unlicensed and 79 GHz for automotive applications. Bandwidth spans depend on targeted radar range resolution but are in the order of up to several GHz, while chirp modulation times vary from dozens of microseconds up to a millisecond.

## 2.1 Sawtooth versus Triangular Wave Linear Chirps

In the recent past, triangle (concatenation of up-chirp and down-chirp) slow FMCW modulation waveforms with typical chirp durations in the millisecond range were dominant. As it will be seen in the next section, the resulting output frequency of an FMCW radar is concurrently influenced by the target's range and its relative radial velocity, thus estimating both parameters simultaneously from a single linear chirp/sweep is an unresolvable task. By using up-slope and down-slope chirps which produce slightly different beat frequencies for an object in motion the two parameters can be decoupled. However, this procedure suffers from ambiguity when there are multiple moving objects and the ghost targets that will appear must be identified and discarded.

In contrast to this, fast sawtooth FMCW modulations which typically last up to a hundred of microseconds automatically resolve object range and velocity into a 2-D image and are in exclusive focus for the rest of the paper.

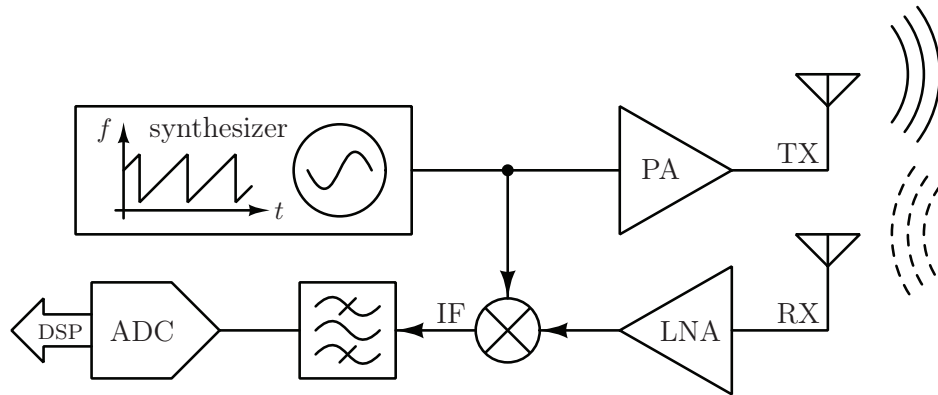


Fig. 2. Simplified high-level block diagram of a typical homodyne FMCW radar which includes linear chirp synthesizer that is being transmitted and used as the local oscillator.

### 3 THE OPERATING PRINCIPLES OF HOMODYNE FMCW RADARS

An FMCW radar transmits a chirp signal defined more closely in the previous section and captures its reflections from objects located in the propagation path. A high-level simplified block diagram of a homodyne FMCW radar is shown in Fig. 2 and features a single transmitter (TX) and a single receiver (RX) antenna. The radar's general operating principles are the following:

- an FMCW synthesizer generates an appropriate chirp signal;
- the generated chirp is first amplified by a power amplifier (PA);
- after amplification the chirp is transmitted by a transmit antenna;
- chirps reflected back from objects are captured by the receive antenna;
- the received signal is then passed through a low-noise amplifier (LNA);
- a down-conversion frequency mixer combines the RX and TX signals at its inputs to produce an intermediate frequency signal at its output;
- the intermediate frequency (IF) signal is also referred to as the beat frequency and it contains information on the irradiated objects/targets.

Additionally, it should be noted that not only the instantaneous output frequency of the down-conversion mixer at any point in time will correspond to the difference of the instantaneous frequencies of the two input signals at that particular point in time, but also the initial phase of the output signal will be equal to the difference between initial phases of the two input signals.

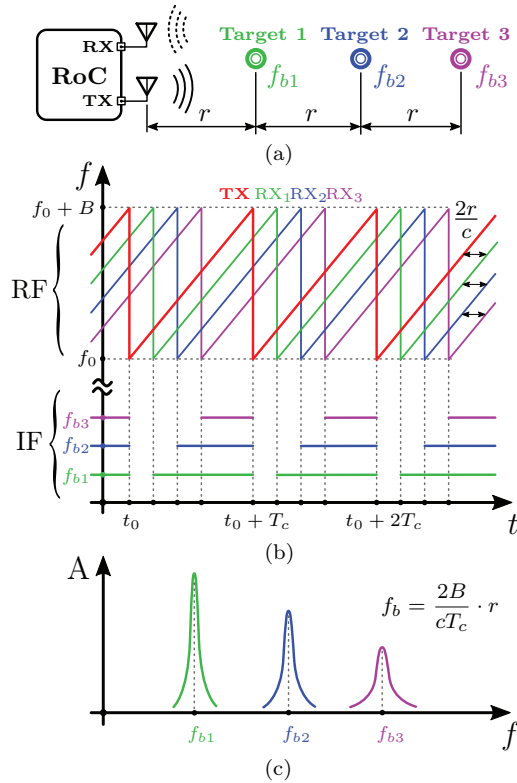


Fig. 3. Static multitarget detection with an FMCW radar (a) spatial object positioning, (b) time-domain transmitted and received reflected up-chirps with the corresponding mixing products (c) amplitude spectrum of appropriately windowed intermediate frequency signal.

It is crucial to remark that the received chirp reflected from a single object is actually just a time-delayed replica of the transmitted chirp. This is best illustrated in Fig. 3 for a somewhat more complicated case of three objects.

Since the mixing product will be the difference of between the instantaneous input frequencies, and since the RF mixer input is just the delayed version of the local oscillator (LO) signal that is being transmitted, hence in the ideal case the IF signal will possess the fixed frequency component proportional to the reflected signal delay. The delay between the transmitted and the received chirp is equal to the round-trip delay  $2r/c$ , where  $r$  denotes the distance between the radar and the object, and  $c$  is the speed of light, while the constant of proportionality will be the transmitted chirp's slope  $S$ .

As a consequence every object that is irradiated by the radar will produce a constant frequency component in the IF signal with the value of  $2rS/c$ .

For the case of a simple stationary or quasi-stationary scene, relation between the beat frequency tone  $f_b$  and the object's range can be related as:

$$f_b = \frac{2rS}{c} = \frac{2B}{cT_c} \cdot r \iff r = \frac{cf_b}{2S} = \frac{cT_c}{2B} \cdot f_b \quad , \quad (4)$$

where chirp slope  $S = B/T_c$  and any radar or object movement is negligible.

Previous statements mean that a single transmitted chirp when reflected from multiple objects located at different distances in front of a radar will also imply multiple received chirps each delayed by a different amount depending on the distance to that particular object. Therefore, the produced IF signal will be composed of several tones that correspond to each of the reflections and the frequency of each is directly proportional to the range of that object.

The initial phase of every component in the IF signal will also be the difference between the phase of the TX chirp and the phase of the RX chirp at the time instant corresponding to the start of the IF signal, or more precisely, to the start of that particular frequency component of the IF signal.

It is important to note that the IF signal is only valid from the time the reflected signal is received at the RX antenna until the end of the current TX chirp. So in order to digitize the IF signal using an ADC, it should be assured that sampling begins after  $2r/c$  time has elapsed after the beginning of the TX chirp, and only up to the time where the TX signal is present.

In practical implementations the round-trip delay is typically just a small fraction of the total chirp duration  $T_c$ , thus the nonoverlapping segment of the transmitted chirp is usually negligible. For example, for an object that is  $r = 150$  m away from the radar and the chirp modulation time of  $T_c = 20 \mu\text{s}$ , this delay accounts only for approximately 5% of the total sweep duration.

### 3.1 Target Distance Estimation and Radar Range Resolution

In a quasi-stationary scene, radial object velocities with respect to a radar are negligible and, as explained, if such a scene is composed out of multiple targets, the produced IF signal will contain multiple frequency components. In other words, the frequency spectrum of such IF signal will reveal multiple tones, the frequency of each being proportional to the distance between each object and the radar. If two objects are closer to each other, or at least at the similar distance from the radar, their tones in the IF signal are also closer.

Certainly the most natural and one of the most popular methods of processing the IF signal is the Fourier transform. It is generally known that longer observation periods yield better frequency resolution so that, for ex-

ample, an observation window of  $T$  seconds in length can independently resolve frequency components that are separated by at least  $1/T$  Hertz.

One of the most important properties of every radar is its range resolution, which refers to the radar's ability to resolve two closely spaced objects. More precisely, it determines the minimum spacing between the two objects which still show up as two separate frequency peaks the IF signal spectrum.

Obviously, one way to improve the range resolution of a radar is to extend the observation window, which looking at Fig. 3 further implies increasing the chirp duration and consequently its bandwidth, if the slope is preserved.

Analytically, two or more distinct IF signal tones can be resolved as long as  $\Delta f > 1/T_c$ , where the small portion at the beginning of the chirp which is associated by the round-trip delay is discarded. It is known that two objects that are spatially  $\Delta r$  apart produce tones separated by  $\Delta f = 2\Delta r S/c$  apart. Eliminating  $\Delta f$  from the previous two expressions and having in mind that the slope  $S = B/T_c$ , the expression for radar's range resolution is obtained:

$$\Delta r > \frac{c}{2ST_c} \implies \Delta r > \frac{c}{2B} \quad , \quad (5)$$

which exclusively depends on the chirp bandwidth  $B$ . Thus, an FMCW radar with a chirp bandwidth of 5 GHz can have a range resolution of 3 cm at least.

Although from Fourier transform properties it may intuitively seem that for the fixed bandwidth  $B$ , chirps of higher duration  $T_c$  would imply longer IF observation windows and better resolving capabilities, the IF signal tones will also be lower in frequency, because of a less steep chirp, and therefore more densely grouped, hence being proportionally harder to differentiate.

Besides range resolution another important parameter is the maximum range of a radar. As high-level block diagram of Fig. 2 indicates, the IF signal is usually filtered and digitized by an analog-to-digital converter (ADC) for further postprocessing inside the following digital signal processing (DSP) chain. So, the maximum detectable distance of a radar  $r_{\max}$  will produce a tone of frequency  $2r_{\max}S/c$  and the ADC's sampling rate should be at least twice as high in order to appropriately discretize this (real) baseband signal.

Viewed the other way around, for the ADC's maximum sampling rate of  $f_s$  the maximum distance that an FMCW radar can see is determined by:

$$r_{\max} = \frac{cf_s}{4S} = \frac{cT_c f_s}{4B} = \frac{cN}{4B} \quad , \quad (6)$$

which follows directly from the sampling theorem for a bandlimited IF signal. Consequently, if it turns out that the ADC's sampling rate presents a bottleneck, the maximum detectable range can always be traded for chirp's slope.

Typically, radars tend to use lower chirp slopes for larger maximum range. Also,  $N$  denotes the number of ADC samples per chirp. The discrete nature of the sampled IF signal suggests the use of discrete Fourier transform (DFT) for further postprocessing. The actual algorithm which is employed is the fast Fourier transform (FFT). Since this processing operation resolves objects in range, it is commonly referred to as the “range-FFT” in radar literature.

It seems appropriate to stress one of the most important benefits of FMCW radars which is also observable from Fig. 3 and that is the difference between the RF bandwidth and the IF bandwidth. Specifically, the RF bandwidth is the frequency range from  $f_0$  up to  $f_0 + B$  which is spanned by the chirp and it directly translates to better range resolution. The typical RF bandwidths are in the order of a few hundred megahertz up to several gigahertz. On the other hand, higher IF bandwidth primarily enables the FMCW radar to see at larger distances and enables faster/steeper chirps. The IF bandwidths are typically in the order of megahertz up to a dozen of megahertz. Hence, the uniqueness of FMCW radar sensors is that huge RF bandwidths do not imply nor necessitate extremely fast data converters.

### 3.2 Radial Velocity Estimation and Radar Velocity Resolution

For the nonstationary case in which there are nonnegligible object or radar movements, all distance measurements through round-trip delay are going to be affected by either signal compression or elongation depending on whether the object is moving away or towards the radar. This effective frequency shift due to relative movement is caused by the well-known Doppler effect.

Small spatial displacements of an object  $\Delta d$  will have an effect on both the IF signal’s frequency and its phase. In mm-wave radars, small displacements are the ones that are comparable to the wavelength which is in the order of several millimeters for typical radar bands. Slight spatial displacements will lead to small round-trip delay changes. Spatial object variation does not have an effect on the initial phase of the received RF signal, but does have on the current phase of the transmitted signal and hence also on the phase of the IF signal. More formally speaking, for very small displacements the higher order terms can be neglected. Furthermore, based on (2) the phase offset of the transmitted signal can be expressed in terms of small displacements as

$$\Delta\phi = 2\pi f_0 \Delta t = 2\pi f_0 \frac{2\Delta d}{c} = \frac{4\pi}{\lambda_0} \cdot \Delta d \quad , \quad (7)$$

where  $\Delta t$  presents the round-trip delay change caused by the object’s range displacement and  $\lambda_0 = c/f_0$  is the wavelength of the transmitted RF signal.

It is crucial to note that the phase of the IF signal changes linearly with small displacements of the object distance and also that the phase is much more sensitive to small spatial perturbations than the actual IF tone frequency. To gain a numerical sense of the previous fact, assume  $\Delta d = \lambda_0/4$  which for typical automotive radar band is in the order of one millimeter. Based on elaborations from the last subsection, every spatial object displacements that are much smaller than the radar's range resolution, which is a few centimeters for present state of the art devices, that is  $\Delta d \ll \Delta r$ , will be practically not discernible in the frequency spectrum. On the other hand the phase changes by  $\Delta\phi = \pi = 180^\circ$  for the quarter wavelength displacements. Thus, the IF signal's phase is very sensitive to small changes in object range.

This gives all the tools for effective velocity measurement of an object by an FMCW radar. The basic idea is to transmit two consecutive chirps of duration  $T_c$ . Each of the two reflected chirps is processed through FFT to detect the range of the object. The range-FFT corresponding to each chirp will have peak at the same location but with a different phase. The measured phase difference of two peaks corresponds to spatial motion of the object.

Assuming that an object with a radial velocity of  $v$  in time  $T_c$  traverses  $\Delta d = vT_c$ , then substituting this into (7) and rearranging it, the object velocity can be directly estimated from the measured phase difference as:

$$v = \frac{\lambda_0}{4\pi T_c} \cdot \Delta\phi \quad . \quad (8)$$

Hence, the phase difference measured across two consecutive chirps can be exploited to estimate the velocity of a single object in front of the radar.

Since the phase difference measurement is unambiguous only in cases in which  $|\Delta\phi < \pi|$ , the maximum unambiguously measurable velocities are:

$$v_{\max} = \frac{\lambda_0}{4T_c} \quad . \quad (9)$$

This further implies that measuring higher  $v_{\max}$  requires faster/shorter chirps.

The previously described method that combines two consecutive chirps does not only work for measuring velocity of a single object, but it is also applicable to multiple objects as well, as long as they are located at different ranges from the radar. However, it will not work if multiple moving objects with different velocities are at the time of measurement all equidistantly located from the radar. This is because the range-FFT of both chirps would yield a single peak whose frequency would correspond to range, but whose phase change would present a combined signal from all of these equi-range object and hence a simple phase comparison technique would not suffice.

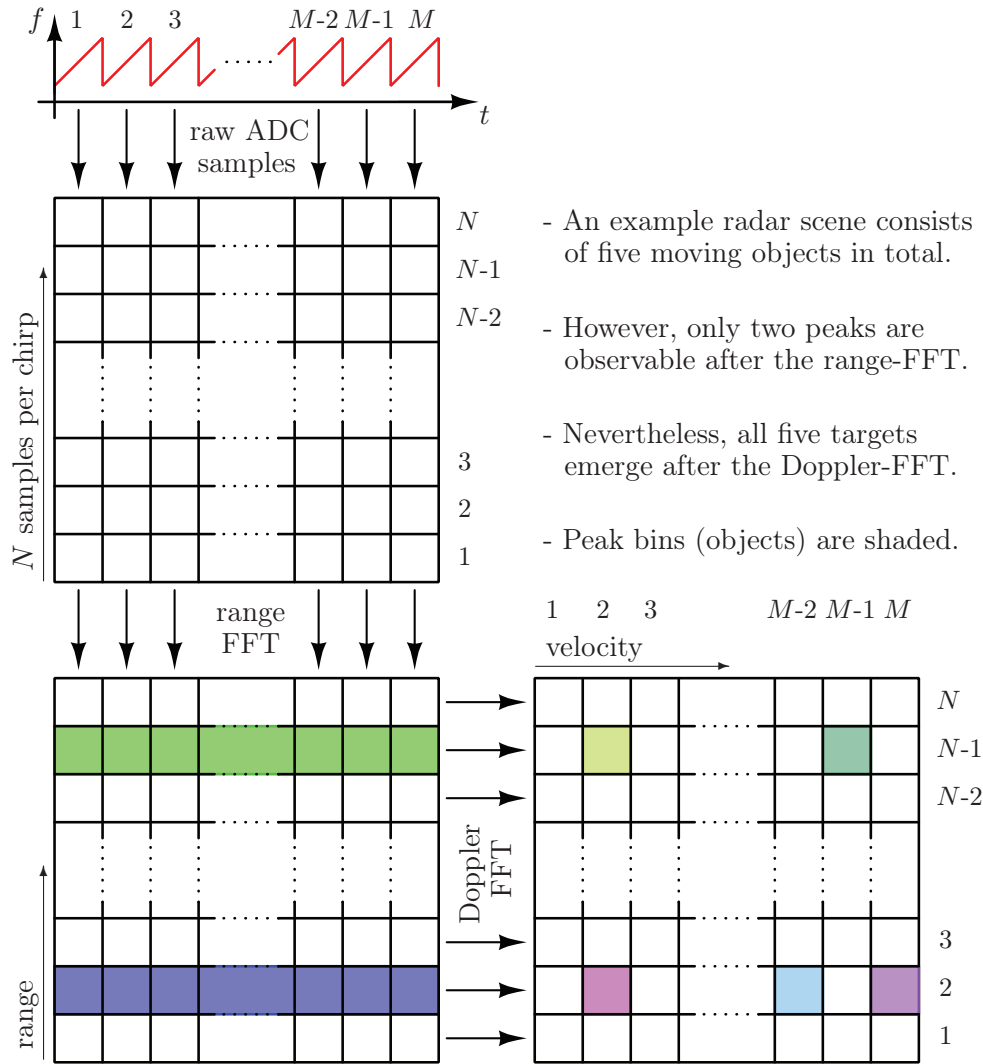


Fig. 4. Two-dimensional (2-D) FFT processing of an FMCW frame containing  $M$  chirps and that  $N$  samples are taken out of each chirp. The first  $M \times N$  matrix contains the raw radar data. After the first FFT which is performed on each matrix column the range is resolved. The second FFT performed across matrix rows resolves the Doppler frequency.

One way of estimating the velocities of multiple equidistant objects is to transmit a series of more than two consecutive equally spaced chirps just as Fig. 4 illustrates. Again, under the assumption of relatively slow motion, the range-FFT corresponding to each of these chirps would yield peaks in identical frequency locations. Nevertheless, the phase of each magnitude peak in

the spectral domain across chirps would be different since it incorporates in itself phase contributions from all of these equidistant objects. Performing yet another FFT round, now across this discrete sequence of chirps would result in peaks corresponding to normalized angular frequencies of each object velocity. The obtained angular frequencies  $\omega$  can be used to back-calculate the object velocities from (8) substituting  $\Delta\phi = \omega$ , i.e., the phase difference between consecutive chirps with the discrete angular frequency. The transform that is performed across chirps is often referred to as the ‘‘Doppler-FFT’’, while the sequence of  $M$  equispaced chirps on which it is performed is called a frame. Therefore, a basic transmission unit of an FMCW radar is the frame.

Just as range estimation capability had its range resolution, the velocity extraction has its own resolution. Analogously to range, there is a certain minimum separation between normalized angular frequencies so that they show up as two independent peaks in the Doppler-FFT spectrum. Identically to the continuous Fourier transform, the longer the DFT input sequence length, better the resolution. More precisely, a sequence of  $M$  samples can resolve discrete angular frequencies that are separated by more than  $2\pi/M$  radians per sample or equivalently  $1/M$  cycles per sample, since one cycle is equal to  $2\pi$  radians. So, in the continuous case, the resolution is inversely proportional to observation time  $T$ , while in the discrete case it is inversely proportional to the number of observed samples  $M$ . Apparently, a way to improve the velocity resolution is to increase the number of chirps per frame.

Analytically, two distinct normalized angular frequencies can be resolved as long as  $\Delta\omega > 2\pi/M$  and since two velocities that are  $\Delta v$  apart produce angular frequencies that are  $\Delta\omega = 4\pi\Delta v T_c/\lambda_0$ , eliminating  $\Delta\omega$  from those expressions and accounting that frame duration is given as  $T_f = MT_c$ , yields

$$\Delta v > \frac{\lambda_0}{2MT_c} \implies \Delta v > \frac{\lambda_0}{2T_f} \quad , \quad (10)$$

where  $T_c$  is the separation between the adjacent chirps. This was an expected result having already mentioned the velocity resolution’s inverse proportionality to frame duration, or, more precisely, the number of chirps in a frame.

Range and velocity estimation is best summarized in Fig. 4 which provides insight in transformations and data organization. Samples taken from an ADC corresponding to each chirp in a frame are stored as the columns of a data matrix. A range-FFT performed on each column resolves objects in range. Subsequently, a Doppler-FFT is performed along the rows of the range-FFT results to resolve objects in the velocity or Doppler dimension.

The process of taking the range-FFT followed by the Doppler-FFT is to-



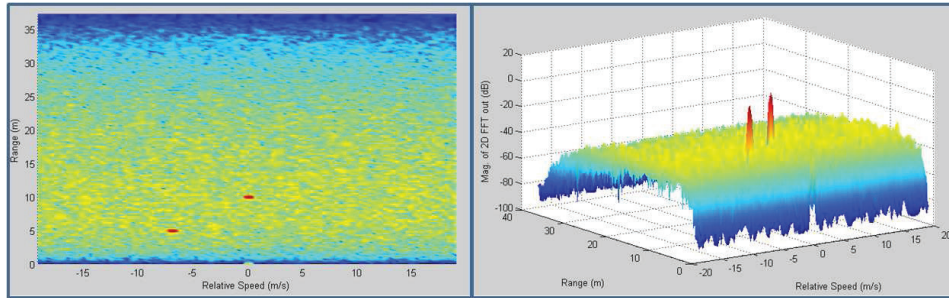


Fig. 6. Radar 2-D FFT images of the so-called range-Doppler response showing range and relative speed/velocity of two point objects that stand out as peaks above the noise floor.

Besides object velocity estimation, measuring IF signal's phase change over multiple antennas separated in space (instead of multiple chirps separated in time) can be used to resolve angular dimension of objects. Differential distance of an object to each antenna is exploited to estimate the angle of arrival. However, extracting target angle information is also not the topic.

Finally, in addition to measuring angle of arrival and object velocity, the fact that the phase of the IF signal is very sensitive to small movements is also the basis for interesting applications such as vibration or heartbeat monitoring, among others. The only assumption is that the movements are small so that the maximum displacement of the object is in the order of a fraction of the  $\lambda_0$  wavelength. Even though the effect on IF frequency tone will be negligible, the phase of the frequency peak will exhibit some sort of a periodic behavior as a response to oscillatory movement of the object. In connection to that, the maximum phase deviation will be related to maximum object displacement providing means to extract the vibration amplitude. In a similar way, the periodicity can be estimated and thus the time evolution of the phase can yield both the amplitude and periodicity of the vibration.

### 3.3 Radar Requirement Mapping to Chirp and Frame Parameters

Having derived the equations that define maximum unambiguously measurable range and velocity, as well as their corresponding resolutions, it is also important to know how to exploit these to design an FMCW transmit signal that meets certain end-user requirements. Assuming the specifications for range resolution ( $\Delta r$ ), maximum range ( $r_{\max}$ ), velocity resolution ( $\Delta v$ ) and maximum velocity ( $v_{\max}$ ) are given and dictated by a certain application, there are multiple strategies how to map this set of requirements to chirp and frame parameters. A sketch of one possible design method is as follows:

- the carrier frequency/wavelength is determined by the frequency band
- chirp bandwidth is directly dictated by  $B = c/2\Delta r$  the range resolution
- inter-chirp time is only ruled by  $T_c = \lambda_0/4v_{\max}$  the maximum velocity
- since both  $B$  and  $T_c$  are fixed, the chirp slope  $S = B/T_c$  is also locked
- the frame duration is governed by  $T_f = \lambda_0/2\Delta v$  the velocity resolution
- finally, it is assumed that the data converter's sampling rate is sufficiently high  $f_s = 4Sr_{\max}/c$  to support IF signal bandwidth of  $2Sr_{\max}/c$ .

However, in practice the process of arriving at desired chirp and frame parameters might involve several iterations, simply because the FMCW radar sensor could have some additional constraints that were not addressed so far.

For example, the maximum IF bandwidth could exceed the ADC's sampling frequency. In such cases, a trade-off between the chirp slope and the maximum measurable distance might be needed. Therefore, in order to increase  $r_{\max}$  the chirp slope would have to be decreased. On the other hand if the modulation time  $T_c$  is frozen based on  $v_{\max}$ , a lower modulation rate  $S$  directly translates to worse range resolution. So, basically, for the fixed modulation time, a short-range radar has a steeper chirp slope and consequently a larger chirp bandwidth and better range resolution, while long-range radar has a lower slope and thereupon a smaller bandwidth and poorer resolution.

Besides the mentioned maximum sampling frequency, other device limitations that are in connection with either analog front-end or digital back-end are often present. For example, there is always a certain maximum slope an FMCW synthesizer can generate. Also related to that, due to a finite settling period, usually a device-specific requirements for idle time between adjacent chirps need to be honored. On the back-end side, the device must have sufficient memory to store the range-FFT output data for all the chirps in the frame to respect a request imposed by the Doppler-FFT on data availability.

#### 4 CONTEMPORARY MM-WAVE FMCW RADAR SENSOR EXAMPLES

Contrary to communication systems where wireless signal receivers are more complicated than their transmitter counterparts, this is not the case with FMCW radar sensors where TX needs to satisfy stringent chirp generation requirements. Namely, although they were not elaborated in the previous sections, object detection quality of FMCW-based sensors will depend on many nonideal effects, such as chirp nonlinearity or synthesizer phase noise.

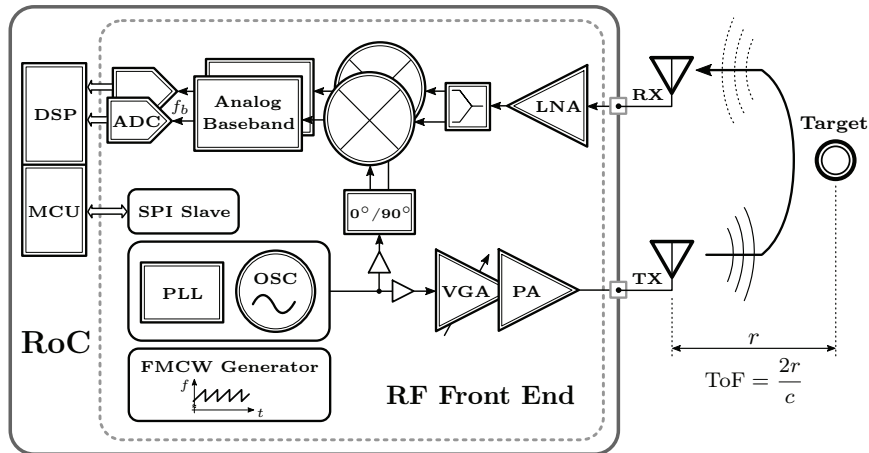


Fig. 7. A contemporary fully-integrated FMCW radar-on-chip (RoC) sensor solution which consists of a single transmitter (TX) and single receiver (RX) antenna and processing chain.

A simplified block diagram of a modern monolithic FMCW radar-on-chip (RoC) sensor is shown in Fig. 7 which sketches its main components. It consists of two major functional blocks: (i) the RF sensor front end containing antennas, signal creation and transmission, signal reception and conditioning and analog-to-digital sampling and conversion, and (ii) digital back end which converts time-domain samples into frequency information, identifies targets and calculates their distances, relative radial velocities, angles and can even perform some advanced functions like target classification or object tracking.

In the mm-wave bands of interest, antennas are mostly realized as patch or dipole antennas on printed-circuit board (PCB) due to their dimensions.

#### 4.1 FMCW Radar Transmitters

The key components of FMCW transmitters are the FMCW synthesizers. They synthesize transmitted radar signal and provide desired modulation schemes. The most important signal conditioning parameters are transmitter phase noise and generated chirp nonlinearity and both have a profound effect on extracting relevant target information from background clutter and noise.

A common block in vast majority of FMCW synthesizers is the oscillator. Integrated voltage-controlled (VCOs) and digitally-controlled oscillators (DCOs) [13] in CMOS and BiCMOS technologies are generally nonlinear with respect to the input control signal due to nonlinear varactor devices [18] which are used in resonators as the frequency control elements. Accordingly,

the biggest issue in an FMCW synthesizer is the compensation of inherent nonlinearity of the DCO/VCO frequency tuning curve. Various methods for FMCW signal generation are proposed so far, each with its own advantages and disadvantages. The most intuitive method is based on the open-loop oscillator, in which the compensation of its nonlinearity is achieved via a look-up table (LUT) and a digital-to-analog converter (DAC). A drawback of this method is the frequency drift with temperature or supply voltage variations which demands periodical updating of the LUT. Apart from aforementioned variations, large effect on the oscillator frequency have unwanted load fluctuations and disturbances which cannot be compensated. Therefore, oscillator nonlinearity is often compensated in the closed-loop systems such as PLLs.

In feedback loop based FMCW synthesizers, dominated by phase-locked loop (PLL) systems, the carrier frequency can be modulated by directly imposing the control signal of a VCO, by modulating the reference frequency of an integer- $N$  PLL [5] or by using fractional- $N$  PLL to change the feedback frequency divider ratio [10–15] hence producing the modulation. Advantages of direct VCO modulation is a simple circuit structure and the absence of additional noise sources. On the other hand, direct VCO modulation requires at least an order of magnitude smaller loop bandwidth in comparison to the modulation frequency which results in a very low filter cross-over frequency, impractical for integration. A method of modulating the reference frequency of integer- $N$  PLL, also known as direct digital frequency synthesis (DDFS), employs LUT and DAC to convert digital word representing phase to analog voltage. The use of DAC constitutes the main disadvantage of this method, because the nonlinearity of the characteristic line, the settling time, the finite slew rate and the jitter coming from the DAC result in spurious signals and serious phase noise performance degradation at the output of the FMCW synthesizer. Probably the most suitable method for FMCW signal generation is based on fractional- $N$  PLLs [25]. This method does not require a low noise DAC nor a LUT, and it provides highly linear frequency sweeps. Thus, it is widely adopted in contemporary integrated FMCW radar sensor modules.

Various frequency synthesizer architectures based on fractional- $N$  PLLs have been reported. They include: a PLL with the fundamental frequency VCO or DCO [5, 10, 12, 13, 26], a PLL with a push-push VCO [27], a PLL and a frequency multiplier [14, 16, 28–30], and a PLL tied with an injection-locked oscillator [31]. Each of these oscillator architectures and methods have their own pros and cons which are summarized in [26]. The choice of the actual synthesizer architecture mainly depends on the required PLL phase noise and output amplitude, but also on the process technology that is being used.

A recent example of an FMCW synthesizer packed in the complete transmitter module [32] provides, in a reasonable modulation time window an extremely large chirp bandwidth of more than 10 GHz thus enabling unmatched range resolutions that are better than 1.5 cm. It is intended to serve as a ubiquitous short-distance radar solution that operates in the unlicensed spectrum band around 65 GHz and to compete in diverse fields of demanding consumer products, like emerging gesture sensors, but also in industrial applications.

Even though at first glance it might seem counterintuitive, excluding the transceiver chain, in particular low-noise and power amplifiers, the short-range radars (SRRs) are actually more challenging to design than the long-range ones. A dominant source of difficulties in SRRs arise due to a limited time frame associated with targets in close proximity to the radar. Specifically, as can be deduced from Fig. 3, for a fixed modulation slope, lower beat frequencies will correspond to objects located at smaller radii. Therefore, it is generally beneficial to decrease the modulation time without compromising the bandwidth in order to push the beat notes of closer targets away from the flicker noise corner frequency. This in turn increases the signal-to-noise ratio (SNR), and consequently the measurement threshold of weaker objects.

Nonlinearity, manifested as an instantaneous frequency deviation from the ideal chirp, disturbs the beat tone and thereby deteriorates radar's measurement accuracy and precision. Even though, faster chirps of high bandwidth, i.e., steeper, are more prone [30] to nonlinear frequency excursions, the above mentioned [32] state-of-the-art radar transmitter is able to achieve the superb frequency sweep linearity under acceptable phase noise levels. Generally speaking, the use of a closed-loop PLL enables the generation of highly linear chirps which avoid smearing of the FFT peaks thus gaining the full benefits of unmatched range resolution associated with high RF bandwidth.

Although a wide RF bandwidth improves radar's range resolution it can typically lead to a longer chirp duration which as a result has a limited maximum unambiguous velocity due to undersampling of the Doppler frequency shift. Hence, supporting steeper chirps, i.e., higher frequency ramp slopes, is essential to achieve higher range resolutions without compromising the maximum velocity. As a side advantage of previous, a wider IF bandwidth relaxes the design of analog baseband filters (moderate roll-off), but requires higher analog-to-digital converter (ADC) sampling rates to achieve equal maximum detectable distances. Another subtle, but also a substantial advantage of steeper modulation slopes is illustrated in Fig. 8, just for the case of triangular chirps, and relates to the fact that spatially equidistant targets yield more separate tones within the beat-frequency domain. Thus, the noise skirt

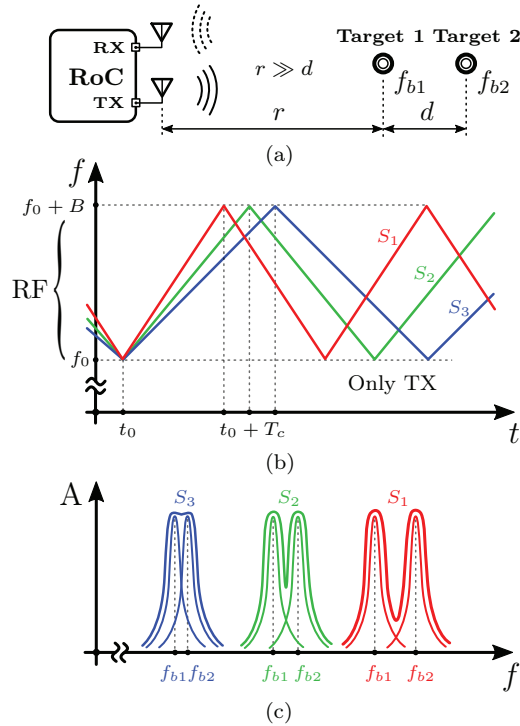


Fig. 8. Effect of the modulation slope  $S$  on the beat frequency separation in static multitarget detection scenarios (a) spatial object positioning, (b) time-domain transmitted FMCW triangular chirps, (c) IF amplitude spectrum for three different modulation rates.

from one target produces less interference in the detection of nearby objects. For stationary targets previous statements can analytically be expressed as:

$$f_{b2} - f_{b1} = \frac{2B}{cT_c} \cdot (r + d) - \frac{2B}{cT_c} \cdot r = \frac{2B}{cT_c} \cdot d = \frac{2}{c} \cdot S \cdot d \quad , \quad (11)$$

where  $d$  is the radial distance between targets with respect to the radar.

Because of all the mentioned reasons it is important to simultaneously increase the RF bandwidth and reduce the modulation time, thus supporting steeper slopes. To achieve that, many technical challenges have to be tackled.

#### 4.2 FMCW Radar Receivers

Although just as important as the transmitter, due to higher similarity to wireless communication transceivers, less attention is devoted to the receiver.

In the simple homodyne implementation, the FMCW receiver is just a plain direct-conversion radio receiver where the modulated signal is frequency

translated in a single conversion step. This avoids additional complexity, but also since the TX and RX frequencies differ yields some properties much alike superheterodyne receiver, e.g., instead of zero the IF is sufficiently large.

Some additional simplifications in terms of LO injection are present, too. Namely, in case of an up-chirp sawtooth modulation the high-side injection is present, while in the case of down-chirp sawtooth modulation the low-side injection applies. For the case of a triangular modulation, both high-side and low-side injection apply to rising and falling frequency slopes, respectively.

Even though the transmitter signal energy can leak through the mixer and then reflect back to create a self-mixing DC offset, the baseband processing chain usually starts with the high-pass filter to alleviate for this effect.

Finally, leading edge FMCW radar sensors adopt the complex baseband receiver architecture which uses quadrature mixers with complex IF and ADC chains that include both in-phase (I) and quadrature (Q) channels. This so-called IQ baseband architecture brings several advantages but the most straightforward one seem to be better noise figure performance (up to 3 dB in theory) because the image band noise foldback to in-band is eliminated. Other benefits include reduced impact of RF intermodulation products due to receiver's nonlinearity combined with the presence of strong TX-to-RX antenna coupling and spillover or very near objects like, e.g., a car bumper.

## 5 CONCLUSIONS

An introduction to radar systems that adopt frequency-modulated continuous waves, or FMCW, to measure range and velocity of remote objects has been made in this article. It has been explained that the received FMCW signal from the remote objects comprises of different time delayed and frequency shifted copies of transmitted chirp signals. An elaborate analysis on how the received signal can be processed in order to obtain the useful information has been performed and the fundamental operating principles of FMCW radars was discussed. Some basic limitations in terms of resolution and maximum measurable distance and speed were shown. Finally, the examples of recent cutting-edge integrated FMCW radar transceiver implementations are given. Since the focus was on the most simple SISO radar sensors, angle-of-arrival estimation, beamforming and MIMO radar techniques were omitted. Also, the so-called radar range equation which is a kind of a link budget for radars, as well as range precision and accuracy were not covered because depending on the actual algorithm it may vary from centimeters down to micrometers. In spite of that, a good head start in the FMCW topic is hopefully provided.

## ACKNOWLEDGEMENTS

The author would like to thank the colleagues from NovelIC Microsystems and Faculty of Engineering, University of Kragujevac on helpful discussions. He would also like to acknowledge support granted by the Ministry of Education, Science and Technological Development through the III-41007 project.

## REFERENCES

- [1] J. Hasch, E. Topak, R. Schnabel, T. Zwick, R. Weigel, and C. Waldschmidt, "Millimeter-wave technology for automotive radar sensors in the 77 GHz frequency band," *IEEE Trans. Microw. Theory Techn.*, vol. 60, no. 3, pp. 845–860, Mar. 2012.
- [2] C. Li, Z. Peng, T. Y. Huang, T. Fan, F. K. Wang, T. S. Horng, J. M. Muñoz-Ferreras, R. Gómez-García, L. Ran, and J. Lin, "A review on recent progress of portable short-range noncontact microwave radar systems," *IEEE Trans. Microw. Theory Techn.*, vol. 65, no. 5, pp. 1692–1706, May 2017.
- [3] M. Pauli, B. Göttel, S. Scherr, A. Bhutani, S. Ayhan, W. Winkler, and T. Zwick, "Miniaturized millimeter-wave radar sensor for high-accuracy applications," *IEEE Trans. Microw. Theory Techn.*, vol. 65, no. 5, pp. 1707–1715, May 2017.
- [4] L. Yujiri, M. Shoucri, and P. Moffa, "Passive millimeter wave imaging," *IEEE Microw. Mag.*, vol. 4, no. 3, pp. 39–50, Sep. 2003.
- [5] T. Mitomo, N. Ono, H. Hoshino, Y. Yoshihara, O. Watanabe, and I. Seto, "A 77 GHz 90 nm CMOS transceiver for FMCW radar applications," *IEEE J. Solid-State Circuits*, vol. 45, no. 4, pp. 928–937, Apr. 2010.
- [6] M. Skolnik, *Introduction to Radar Systems*, 3rd ed. McGraw-Hill, 2002.
- [7] S. Trotta, H. Knapp, D. Dibra, K. Aufinger, T. F. Meister, J. Bock, W. Simburger, and A. L. Scholtz, "A 79 GHz SiGe-bipolar spread-spectrum TX for automotive radar," in *IEEE Int. Solid-State Circuits Conf. (ISSCC) Dig. Tech. Papers*, Feb. 2007, pp. 430–613.
- [8] D. Guermandi, Q. Shi, A. Dewilde, V. Derudder, U. Ahmad, A. Spagnolo, I. Ocket, A. Bourdoux, P. Wambacq, J. Craninckx, and W. V. Thillo, "A 79-GHz  $2 \times 2$  MIMO PMCW radar SoC in 28-nm CMOS," *IEEE J. Solid-State Circuits*, vol. 52, no. 10, pp. 2613–2626, Oct. 2017.
- [9] W. V. Thillo, V. Giannini, D. Guermandi, S. Brebels, and A. Bourdoux, "Impact of ADC clipping and quantization on phase-modulated 79 GHz CMOS radar," in *2014 11th Eur. Radar Conf. (EuRAD)*, Oct. 2014, pp. 285–288.
- [10] J. Lee, Y. A. Li, M. H. Hung, and S. J. Huang, "A fully-integrated 77-GHz FMCW radar transceiver in 65-nm CMOS technology," *IEEE J. Solid-State Circuits*, vol. 45, no. 12, pp. 2746–2756, Dec. 2010.

- [11] N. Pohl, T. Jaeschke, and K. Aufinger, "An ultra-wideband 80 GHz FMCW radar system using a SiGe bipolar transceiver chip stabilized by a fractional- $N$  PLL synthesizer," *IEEE Trans. Microw. Theory Techn.*, vol. 60, no. 3, pp. 757–765, Mar. 2012.
- [12] T. N. Luo, C. H. E. Wu, and Y. J. E. Chen, "A 77-GHz CMOS FMCW frequency synthesizer with reconfigurable chirps," *IEEE Trans. Microw. Theory Techn.*, vol. 61, no. 7, pp. 2641–2647, Jul. 2013.
- [13] W. Wu, R. B. Staszewski, and J. R. Long, "A 56.4-to-63.4 GHz multi-rate all-digital fractional- $N$  PLL for FMCW radar applications in 65 nm CMOS," *IEEE J. Solid-State Circuits*, vol. 49, no. 5, pp. 1081–1096, May 2014.
- [14] J. Park, H. Ryu, K. W. Ha, J. G. Kim, and D. Baek, "76-81-GHz CMOS transmitter with a phase-locked-loop-based multichirp modulator for automotive radar," *IEEE Trans. Microw. Theory Techn.*, vol. 63, no. 4, pp. 1399–1408, Apr. 2015.
- [15] G. Hasenaecker, M. van Delden, T. Jaeschke, N. Pohl, K. Aufinger, and T. Musch, "A SiGe fractional- $N$  frequency synthesizer for mm-wave wide-band FMCW radar transceivers," *IEEE Trans. Microw. Theory Techn.*, vol. 64, no. 3, pp. 847–858, Mar. 2016.
- [16] J. H. Song, C. Cui, S. K. Kim, B. S. Kim, and S. Nam, "A low-phase-noise 77-GHz FMCW radar transmitter with a 12.8-GHz PLL and a  $\times 6$  frequency multiplier," *IEEE Microw. Compon. Lett.*, vol. 26, no. 7, pp. 540–542, Jul. 2016.
- [17] H. Jia, L. Kuang, W. Zhu, Z. Wang, F. Ma, Z. Wang, and B. Chi, "A 77 GHz frequency doubling two-path phased-array FMCW transceiver for automotive radar," *IEEE J. Solid-State Circuits*, vol. 51, no. 10, pp. 2299–2311, Oct. 2016.
- [18] I. M. Milosavljević, Đ. P. Glavonjić, D. P. Krčum, L. V. Saranovac, and V. M. Milovanović, "A highly linear and fully-integrated FMCW synthesizer for 60 GHz radar applications with 7 GHz bandwidth," *Springer Analog Integr. Circuits Signal Process.*, vol. 90, no. 3, pp. 591–604, Mar. 2017.
- [19] M. Hitzler, S. Saulig, L. Boehm, W. Mayer, W. Winkler, N. Uddin, and C. Waldschmidt, "Ultracompact 160-GHz FMCW radar MMIC with fully integrated offset synthesizer," *IEEE Trans. Microw. Theory Techn.*, vol. 65, no. 5, pp. 1682–1691, May 2017.
- [20] A. Townley, P. Swirhun, D. Titz, A. Bisognin, F. Gianesello, R. Pilard, C. Luxey, and A. M. Niknejad, "A 94-GHz 4TX-4RX phased-array FMCW radar transceiver with antenna-in-package," *IEEE J. Solid-State Circuits*, vol. 52, no. 5, pp. 1245–1259, May 2017.
- [21] E. Öztürk, D. Genschow, U. Yodprasit, B. Yilmaz, D. Kissinger, W. Debski, and W. Winkler, "A 60-GHz SiGe BiCMOS monostatic transceiver for FMCW radar applications," *IEEE Trans. Microw. Theory Techn.*, vol. 65, no. 12, pp. 5309–5323, Dec. 2017.

- [22] Federal Communications Commission (FCC), "Operation within the band 57-71 GHz, Title 47 CFR Part 15, Subpart C, §15.255," Nov. 2016.
- [23] B. P. Ginsburg, K. Subburaj, S. Samala, K. Ramasubramanian, J. Singh, S. Bhatara, S. Murali, D. Breen, M. Moallem, K. Dandu, S. Jalan, N. Nayak, R. Sachdev, I. Prathapan, K. Bhatia, T. Davis, E. Seok, H. Parthasarathy, R. Chatterjee, V. Srinivasan, V. Giannini, A. Kumar, R. Kulak, S. Ram, P. Gupta, Z. Parkar, S. Bhardwaj, Y. C. Rakesh, K. A. Rajagopal, A. Shrimali, and V. Rentala, "A multimode 76-to-81 GHz automotive radar transceiver with autonomous monitoring," in *IEEE Int. Solid-State Circuits Conf. (ISSCC) Dig. Tech. Papers*, Feb. 2018, pp. 158–160.
- [24] V. Winkler, "Range Doppler detection for automotive FMCW radars," in *Proc. Eur. Radar Conf.*, Oct. 2007, pp. 166–169.
- [25] W. Wang, X. Chen, and H. Wong, "A system-on-chip 1.5 GHz phase locked loop realized using 40 nm CMOS technology," *Facta Universitatis, Series: Electronics and Energetics*, vol. 31, no. 1, pp. 101–113, Mar. 2018.
- [26] S. Kang, J. C. Chien, and A. M. Niknejad, "A W-band low-noise PLL with a fundamental VCO in SiGe for millimeter-wave applications," *IEEE Trans. Microw. Theory Techn.*, vol. 62, no. 10, pp. 2390–2404, Oct. 2014.
- [27] A. Ergintav, Y. Sun, F. Herzel, H. J. Ng, G. Fischer, and D. Kissinger, "A 61 GHz frequency synthesizer in SiGe BiCMOS for 122 GHz FMCW radar," in *Proc. Eur. Microw. Integr. Circuits Conf.*, Oct. 2016, pp. 325–328.
- [28] G. Liu, A. Trasser, and H. Schumacher, "A 64-84-GHz PLL with low phase noise in an 80-GHz SiGe HBT technology," *IEEE Trans. Microw. Theory Techn.*, vol. 60, no. 12, pp. 3739–3748, Dec. 2012.
- [29] H. J. Ng, A. Fischer, R. Feger, R. Stuhlberger, L. Maurer, and A. Stelzer, "A DLL-supported, low phase noise fractional- $N$  PLL with a wideband VCO and a highly linear frequency ramp generator for FMCW radars," *IEEE Trans. Circuits Syst. I, Reg. Papers*, vol. 60, no. 12, pp. 3289–3302, Dec. 2013.
- [30] J. Vovnoboy, R. Lvinger, N. Mazor, and D. Elad, "A dual-loop synthesizer with fast frequency modulation ability for 77/79 GHz FMCW automotive radar applications," *IEEE J. Solid-State Circuits*, vol. 53, no. 5, pp. 1328–1337, May 2018.
- [31] A. Musa, R. Murakami, T. Sato, W. Chaivipas, K. Okada, and A. Matsuzawa, "A low phase noise quadrature injection locked frequency synthesizer for mm-wave applications," *IEEE J. Solid-State Circuits*, vol. 46, no. 11, pp. 2635–2649, Nov. 2011.
- [32] I. M. Milosavljević, D. P. Krčum, D. P. Glavonjić, S. P. Jovanović, V. R. Mihajlović, D. M. Tasovac, and V. M. Milovanović, "A SiGe highly integrated FMCW transmitter module with a 59.5-70.5 GHz single sweep cover," *IEEE Trans. Microw. Theory Techn.*, vol. 66, no. 9, pp. 4121–4133, Sep. 2018.